Synthesis and biological evaluation of cholic acid-conjugated oxaliplatin as a new prodrug for liver cancer

Jing Jiang [a,1], Fuguo Han [b,1], Kaixuan Cai [c,1], Qiushuo Shen [d], Cuiping Yang [d], Anli Gao [a], Juan Yu [a], Xuemei Fan [b], Yanli Hao [b], Zhao Wang [b], Weiping Liu [a,*], Yun Shi [c,**], Qingfei Liu [b,***]

[a] Kunming Institute of Precious Metals, Kunming 650106, China
[b] School of Pharmaceutical Science, Tsinghua University, Beijing 100084, China
[c] Dongzhimen Hospital, Beijing University of Chinese Medicine, Beijing 100700, China
[d] Kunming Institute of Zoology, Chinese Academy of Sciences, Kunming 650201, China

ARTICLE INFO

ABSTRACT

A cholic acid-conjugated oxaliplatin, LLC-202, is developed as a novel prodrug for liver cancer. The conjugate is obtained by using 3-NH$_2$_cyclobutane-1,1-dicarboxylate as a linker between the oxaliplatin analogue and cholic acid moiety and cholic acid is strongly bonded to the linker via an amide bond. Pharmacokinetic experiment shows that LLC-202 is mainly distributed and accumulated in the liver after intravenous administration to Sprague-Dawley rats, revealing the liver-targeting profile. Compared to oxaliplatin, LLC-202 is more easily taken up by human liver cancer cells than normal human liver cells. LLC-202 exhibits higher in vitro anticancer activity and higher efficacy comparable to oxaliplatin in treating primary hepatocellular carcinoma in C57BL/6 mice. It can significantly prolong the survival time of tumor-bearing mice by inducing apoptosis and inhibiting proliferation of cancer cells. In addition, LLC-202 shows less cytotoxicity toward normal human liver cells than oxaliplatin. Its acute toxicity in healthy Kunming (KM) mice after i.v. administration is comparable to oxaliplatin. Histopathological examination reveals that the main toxicity of LLC-202 in mice is the depression of bone marrow hematopoietic cells. The results suggest that LLC-202 has great potential for further development as a new prodrug specific for liver cancer.

1. Introduction

Primary liver cancer (hepatocellular carcinoma, HCC) is the sixth most frequent cancer type and the second-highest cause of cancer-related death worldwide [1]. It has been particularly prevalent in China because of the high prevalence of chronic hepatitis B infection. Chinese HCC patients account for more than half of the world's total cases, causing 422,000 deaths in China in 2015, only second to the mortality of lung cancer [2]. Due to its insidious symptoms at early stages and difficulty in early detection, most patients are diagnosed at an advanced stage. Therefore, systemic therapy based on anticancer drugs is an important option for these advanced cancer patients, but the survival benefits of chemotherapy are usually minimal [3,4]. Oxaliplatin plus fluorouracil (FU) and leucovorin (LV) (FOLFOX4) was approved for the systemic treatment of advanced HCC patients in China and both overall survival and progression-free survival can be improved compared to treatment with doxorubicin (DOX) [5,6].

Platinum-based drugs, represented by cisplatin, carboplatin and

oxaliplatin, are among the few chemotherapeutic agents effective against liver cancer [7]. Oxaliplatin is particularly a third-generation platinum antitumor drug, approved by the US FDA in 2002 following cisplatin and carboplatin, and has been used mainly in the combination chemotherapy of metastatic colorectal cancer [8]. More recently, it was approved first in China for the first-line treatment of inoperable, locally advanced and metastatic liver cancer after several clinical trials which had demonstrated its superiority over cisplatin in prolonging survival and reducing the risk of death of patients with advanced liver cancer [9]. In addition, oxaliplatin has synergistic anticancer effects with targeted therapy and immunotherapy against HCC [10,11]. However, the efficacy and applicability of oxaliplatin, like other cytotoxic anticancer agents, is often compromised by the substantial risk for severe toxicities, due to their poor specificity of tumor targeting [12]. Therefore, tumor targeting has become a highly active field of research for anticancer drugs, for it can deliver the drugs directly to tumor sites and decrease the drug-related toxicities, resulting in an increase of chemotherapy efficiency.

Cholic acid, as a fundamental component for synthesis of bile acid in the liver, is taken up and used mainly by hepatocytes. It has been shown that hepatic epithelial cells express a few transport proteins that take up bile salts from the bloodstream, leading to the suggestion that this steroid could be used as a carrier molecule to shuttle drugs to the liver [13–16]. For example, conjugate of cholic acid and fluorouracil had a longer half-life and significantly increased fluorouracil concentrations in liver tissue [17]. Cisplatin-ursodeoxycholic derivative (Bamet-UD2) could enhance cytostatic activity versus liver tumors. Studies with rat hepatocytes and isolated rat livers confirmed that the resulting complex Bamet-R2 was taken up by the pathway naturally used for bile acid uptake, and is secreted into the bile [18]. Furthermore, bile acid receptors such as farnesoid X receptor (FXR, NR1H4) have been recently reported as targets for drug development [19]. Conjugated with bile acids or their derivatives, drugs can target HCC cells through the bile acid transport system, so it is an ideal delivery molecule for drugs to target the liver [20]. For example, three conjugates of cytarabine and cholic acid showed good liver-targeting properties and absorption, as compared with cytarabine [21]. Cisplatin, the first classic platinum-based anticancer drug, has led researchers worldwide to developing numerous cisplatin analogs to overcome its severe toxicity and resistance, and improve its cancer-targeting features. Using bile acids as targeting carriers for delivering platinum-related cytostatic agents such as cisplatin to liver tumors, several bile acid derivatives, which have a platinum atom as the DNA-reactive part, have been synthesized and their liver organotropism has been investigated [22–25]. A series of bile acid derived Pt complexes reported by literature is shown in Table 1.

With more detailed discovery of the structure and transport mechanism of bile acid receptors and transporters, as well as synergistic effect, bile acids have proven to be inspiring tools in the design of pharmacological applications with a vast number of objectives [36–39].

However, our concern is that the conjugate via monodentate Pt-OOC coordination bonds, from the perspective of coordination chemistry, may not be stable enough in aqueous solutions for a drug candidate, and that bile acid ligands will dissociate readily from the platinum (II) center before the complex finally arrives at the liver. An alternative means of linking a bile acid to a platinum (II) drug involved conjugation to a non-leaving group ligand as a linker to improve the stability of the conjugate and such a cholic acid-carboplatin compound (CarboChAPt) with chemical formula of [Pt(Cyclobutane-1,1-dicarboxylato){CholCOO $(CH_2)_nCH-(CH_2NH_2)_2$}], displayed activity in cultured cells by a mechanism of action similar to that of cisplatin [27,28].

With a view to using cholic acid as a targeting carrier for delivering platinum anti-cancer drugs to the liver tumor site, a new coupling way has been adopted in our studies for attaching cholic acid to an oxaliplatin analogue via cyclobutane-1,1-dicarboxylic acid (CBDA), in order to develop a new cholic acid-mediated oxaliplatin prodrug for targeting the liver tumor. The resulting compound LLC-202 (meaning the 202th

compound of Liu lab) (Fig. 1) consisted of a hybrid of oxaliplatin and carboplatin, which is very effective against hepatocellular carcinoma, 1,1-cyclobutane- dicarboxylic acid as the linker, and cholic acid as the liver-targeting moiety. For oxaliplatin, a dose-limiting side-effect is believed to be due to oxalate, a leaving group as well as one of the metabolites of oxaliplatin, since $C_2O_4^{2-}$ can form an insoluble salt with Ca^{2+} (CaC_2O_4), leading to the depletion via Ca^{2+} and/or Mg^{2+} in the cells [40–42]. LLC-202 does not contain oxalate in its structure and is therefore expected to avoid the neurotoxicity caused by oxalate. All these positive results support further evaluation and development of LLC-202. In the present paper, we will mainly report its chemical synthesis, pharmacodynamics, and toxicity, as well as its pharmacokinetics.

2. Experimental section

2.1. General information

Potassium tetrachloroplatinate (II), a starting material, was purchased from Alfa Aesar. Oxaliplatin was provided by the Kunming Guiyan Pharmaceutical Co. All other chemicals obtained from commercial suppliers were of analytical grade, and used as received. Water was distilled prior to use. The synthetic procedures were carried out in a light-protected environment when platinum complexes were involved. Composition analyses for C, H and N were performed with a Carlo-Ebra instrument, whereas the content of platinum was analyzed according to the method in European Pharmacopoeia (EP) 6.5: Ignite an empty porcelain crucible fitted with a lid in a furnace at 800° for 30 min. Cool in a desiccator, and weigh. Add 500 mg of the sample, weigh, to the crucible, and ignite in a furnace by stepwise increments as follows. Introduce into the furnace and increase the temperature to 200° within 15 min, then to 400° within 15 min, then to 600° within 15 min, then finally to 800° within 15 min. Allow to remain in the furnace at 800° for 30 min. Remove, cool in a desiccator, and reweigh. Calculate the percentage of platinum in the portion of Oxaliplatin taken: $Result = \frac{W_2 - W_1}{W_0} \times 100\%$, where W_1 is the weight of empty crucible after igniting for 30 min (g), W_0 is the weight of sample (g) and W_2 is the weight of sample and crucible after igniting for 30 min (g). FT-IR spectra were measured in KBr pellets with a Perkin Elmer 880 spectrometer. ^1HNMR and $^{13}CNMR$ spectra were recorded in dimethyl sulfoxide (DMSO) on Bruker AV-400 MHz instrument relative to TMS (tetramethylsilane) as an external standard. Electrospray mass spectra were recorded on an Agilent G6230 TOF mass spectrometer.
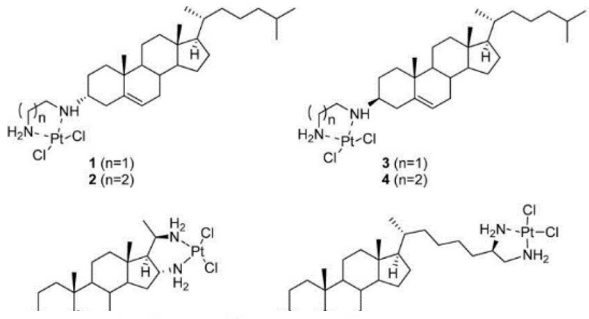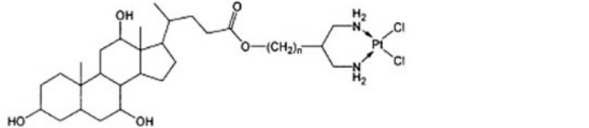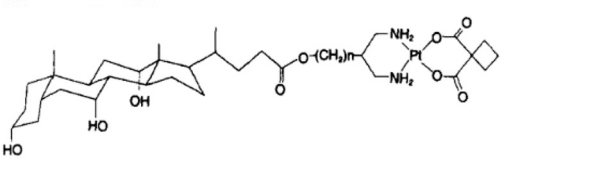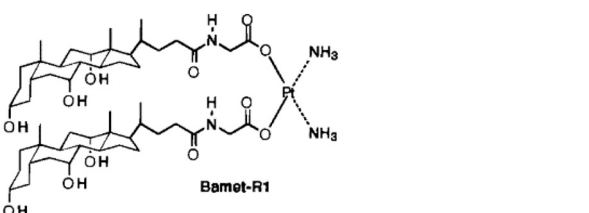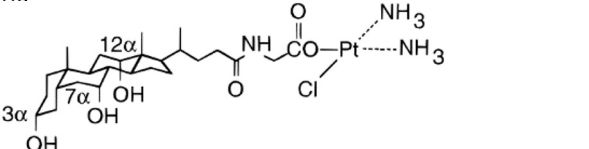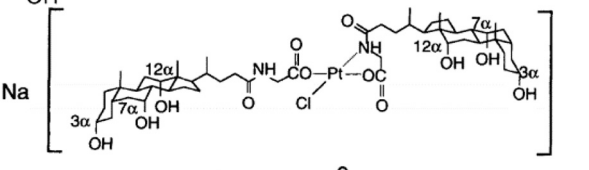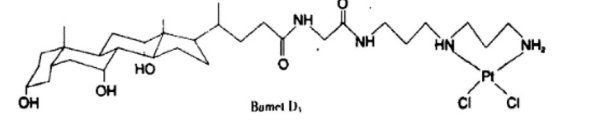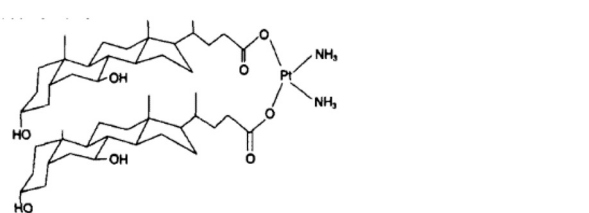
2.2. Chemical synthesis of LLC-202

2.2.1. Diethyl 3-TsO-1,1-cyclobutane diethyl dicarboxylate (2)

Under nitrogen protection, 5.1 g (0.024 mol) of diethyl 3-hydrxoy-1,1-cyclobutane dicarboxylate (1), 9.6 g (0.094 mol, 4 eq.) of triethylamine (Et₃N) and 0.58 g (0.0047 mol, 20% eq.) of 4-dimethylaminopyridine (DMAP) were added to 10 mL of dichloromethane, mixed and dissolved, and immersed with 9.0 g (0.047 mol, 2 eq.) para-toluensulfonyl chloride (TsCl) and 10 mL dichloromethane mixture in an ice bath. After stirring overnight at room temperature, the progress of the reaction was monitored to completion by thin-layer chromatography (TLC), with a developing solvent consisting of petroleum ether / ethyl acetate (4/1), $R_f = 0.4$. The whole mixture was purified by column chromatography separation eluting with petroleum ether / ethyl acetate (6/1) to give 2. Yield 8.2 g (94%).

2.2.2. Diethyl 3-azido-1,1-cyclobutane dicarboxylate (3)

Under nitrogen protection, 8.0 g (0.022 mol) 2, 4.2 g (0.065 mol, 3 eq.) sodium azide (NaN₃), and 7.3 g (0.022 mol, 1 eq.) Bu₄NHSO₄ were dissolved in 10 mL dimethyl formamide (DMF), and stirred at 80 °C overnight. The mixture was stirred at reflux and cooled to room temperature, transferred to a 1 L separatory funnel, and after addition of

Table 1

A series of bile acid derived Pt complexes reported by literature.

Bile acid derived Pt complexes	References
	[26]
	[27]
	[28]
	[29]
	[30]
	[22,31]
	[32]

(continued on next page)

Table 1 (*continued*)

Bile acid derived Pt complexes	References

Lithocholic acid: $R_1 = R_2 = R_3 = H$
Deoxycholic acid: $R_1 = R_2 = H$, $R_3 = OH$
Hyodeoxycholic acid: $R_1 = OH$, $R_2 = R_3 = H$
Cholic acid: $R_1 = H$, $R_2 = R_3 = OH$

[33]

3: R = OH
6: R = OAc
(*S*)-configuration

[34]

R   S

R   S

plenty of water, extracted twice with 100 mL ethyl acetate each. The ethyl acetate was washed three times with 100 mL saturated salt water each, and dried with anhydrous sodium sulfate. The progress of the reaction was monitored to completion by TLC, with a developing solvent of petroleum ether / ethyl acetate (10/1), $R_f = 0.5$. The whole mixture was purified by column chromatography separation eluting with petroleum ether / ethyl acetate (10/1) to give 3. Yield 3.3 g (64%).

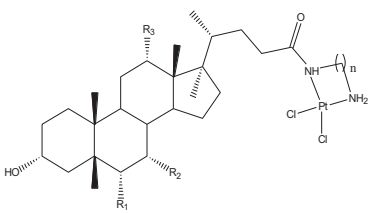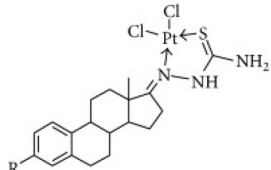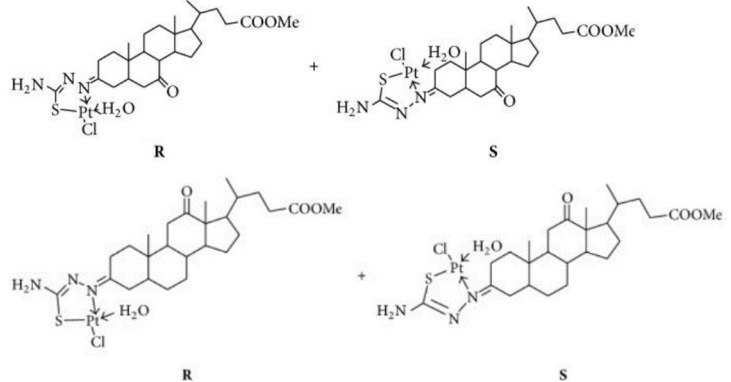*2.2.3. Diethyl 3-amino-1, 1-cyclobutane dicarboxylate (4)*

Compound 3 (5.0 g) was dissolved in 150 mL ethyl acetate and 1.0 g (20% eq.)10% Pd/C. H_2 was added and the reaction was performed overnight at room temperature under normal pressure. The mixture was filtered and concentrated directly to give 10 g 4. Yield 96%.

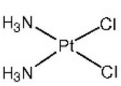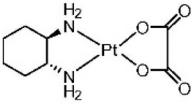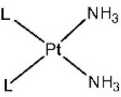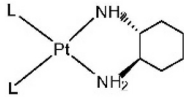*2.2.4. 3-Cholic amide 1,1-cyclobutane dicarboxylic acid diethyl ester (5)*
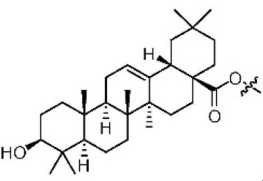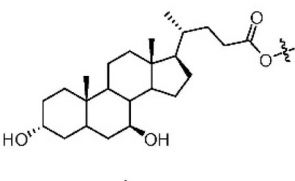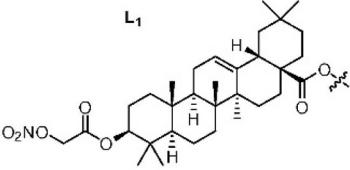
First, 1.1 g (5.25 mmol, 1.05 eq.) dicyclohexylcarbodiimide (DCC) was dissolved in 5 mL tetrahydrofuran, and placed in a fridge to cool, and set aside. Then, 2.0 g (5 mmol, 1 eq.) cholic acid (represented by RCOOH) was dissolved in 10 mL tetrahydrofuran, stirred to dissolve, cooled in an ice salt bath to about −15 °C. To the mixture we added 0.77 g (5 mmol, 1 eq.) 1-hydroxybenzotriazole (HOBt), 1.1 g (5 mmol) 4, and 0.55 mL *N*-methylmorpholine (NMM), stirred for 1–2 min and poured the mixture into the cooled DCC tetrahydrofuran solution, stirred for 2 h

below −15 °C, naturally recovered to room temperature, and stirred overnight. The mixture was filtrated to remove an insoluble white solid, and then tetrahydrofuran was removed by vacuum rotation to obtain a yellow viscous liquid. The liquid was dissolved in dichloromethane, and washed three times in turn with a saturated $NaHCO_3$ solution, a 10% citric acid solution, a saturated $NaHCO_3$ solution and a saturated NaCl solution. The organic layer was collected, dried over anhydrous Na_2SO_4, filtrated to remove desiccant, concentrated, ground and solidified with petroleum ether, and filtrated to obtain a white solid. The progress of the reaction was monitored to completion by TLC, using a developing solvent of petroleum ether / ethyl acetate / ethyl alcohol (4/4/1), $R_f = 0.5$. The whole mixture was purified by column chromatography separation, eluting with petroleum ether / ethyl acetate / ethyl alcohol (4/4/1) to give 5. Yield 2.0 g (66%).

2.2.5. 3-Cholic amide-1,1-cyclobutane dicarboxylic acid (6)

First, 0.6 g (0.015 mol, 2.6 eq.) NaOH and 50 mL water were added to a 250 mL reaction flask, stirred to dissolve, dropped into a mixed solution of 5 (3.5 g,0.0058 mol) and 100 mL methanol, and then mixed at 50 °C for 8 h. The progress of the reaction was monitored to completion by TLC. Then, 2 g activated carbon was added, stirred for 30 min, filtrated and evaporated under vacuum to remove methanol. The water layer was extracted twice with ethyl acetate (50 mL each time) to

Table 1 (*continued*)

Bile acid derived Pt complexes	References

Cisplatin

Oxaliplatin

1a, L= L$_1$;
1c, L= L$_2$;
1e (Bamet-UD2), L= L$_3$

1b, L= L$_1$;
1d, L= L$_2$;
1f, L= L$_3$

L$_1$:oleanolic acid

[35]

L$_1$

L$_3$

L$_2$

L$_2$:oleanolic acid -NO
L$_3$:ursodeoxycholic acid

remove organic impurities. The water layer was separated, adjusted to pH 1.0 with diluted hydrochloric acid, and extracted three times with ethyl acetate (60 mL each time). The organic layer was combined, washed three times with saturated salt water (60 mL each time), dried with anhydrous sodium sulfate and reduced pressure to produce a white product. The progress of the reaction was monitored to completion by TLC, with a developing solvent of petroleum ether / ethyl acetate / formic acid (10/15/2), R$_f$ = 0.3. The whole mixture was purified by column chromatography separation, eluting with petroleum ether / ethyl acetate / formic acid (10/15/2) to give 6. Yield 2.4 g (76%). The purity was determined by High performance liquid chromatography (HPLC) to be >95%. MS: 549.69 (C$_{30}$H$_{47}$NO$_8$). ^{1}H NMR (500 MHz, DMSO): δ_H 4.20–4.16 (m, 1H, H-25), 4.08 (s, 1H, OH), 3.99 (s, 1H, OH), 3.77 (s, 1H, H-12), 3.59 (s, 1H, H-7), 3.20–3.17 (m, 1H, H-3), 2.57 (t, 2H, J = 10.0 Hz, H-26), 2.29 (t, 2H, J = 9.0 Hz, H-29), 2.21–2.10 (m, 2H, H-4a, H-9), 2.04–1.89 (m, 3H, H-23a, H-14, H-23b), 1.80–1.56 (m, 6H, H-6a, H-17, H-16a, H-15a, H-1a, H-22a), 1.46 (1H, m, H-4b), 1.42–1.10 (m, 10H, H-11a, H-2a, H-6b, H-11b, H-8, H-2b, H-20, H-5, H-22b, H-16b), 0.95–0.93 (m, 1H, H-15b), 0.90 (1H, d, J = 6.5 Hz, H-21), 0.85–0.82 (m, 1H, H-1b), 0.79(3H, s, H-19), 0.56(3H, s, H-18); ^{13}C NMR (100 MHz, CDCl$_3$) δ_C: 35.3 (CH$_2$, C-1), 30.4 (CH$_2$, C-2), 70.5 (CH, C-3), 39.6 (CH$_2$, C-4), 41.5 (CH, C-5), 34.9 (CH$_2$, C-6), 66.3 (CH, C-7), 39.4 (CH, C-8), 26.2 (CH, C-9), 34.4 (C, C-10), 28.6 (CH$_2$, C-11), 71.0 (CH, C-12), 45.8 (C, C-13), 41.4 (CH, C-14), 22.8 (CH$_2$, C-15), 27.3 (CH$_2$, C-16), 46.1 (CH, C-17), 12.4 (CH$_3$, C-18), 22.6 (CH$_3$, C-19), 35.2 (CH, C-20), 17.1 (CH$_3$, C-21), 31.6 (CH$_2$, C-22), 32.5 (CH$_2$, C-23), 172.0 (C, C-24), 38.4 (CH, C-25), 36.9 (CH$_2$, C-26), 46.6 (C, C-27), 173.1 (C, C-28), 36.9 (CH$_2$, C-29), 172.5 (C, C-30).

2.2.6. LLC-202

An aqueous solution of cis-[Pt(*1R,2R*-diaminocyclohexane)(H$_2$O)$_2$] (NO$_3$)$_2$ was prepared according to the literature [43]. After 6 (2.4 g, 4.4 mmol) was dissolved in 88 mL NaOH (0.1 M), it was mixed with cis-[Pt (*1R,2R*-diaminocyclohexane)(H$_2$O)$_2$] (NO$_3$)$_2$ (4.8 mmol, excess 10%) and stirred for 12 h. A white precipitate was formed and collected. After being washed with water 3 times, the product was vacuum freeze-dried to give the desired product. It was purified by first dissolving in 250 ml DMF, filtrating the insoluble impurities, and then adding 3.0 L water to re-precipitate the sample for structural characterization and biological tests. Yield 2.7 g (71%). Calcd. % for C$_{36}$H$_{60}$N$_3$O$_8$Pt: C, 50.5; H, 6.89; N, 4.91; Pt, 22.8. Found: C, 50.2; H, 6.919; N, 4.90; Pt, 22.6. HRESI$^+$-MS: [M + Na] $^+$ *m/z* Calcd. = 879.3848 (^{194}Pt), Found = 879.3857. MS (ESI$^+$) m/z, 857([MH] $^+$). IR (KBr, cm^{-1}): 3440 (s, vO-H), 3256 (s, vN-H), 1721(m, vC = 0), 1633(vs, vas (COO)), 1385(s, va(COO)). ^{1}H NMR (400 MHz, DMSO-*d$_6$*) δ_H: 5.90–5.85 (m, 2H, NH$_2$), 5.20–5.15(m, 2H, NH$_2$), 4.32 (s, 1H, H-OH), 4.09 (s, 1H, H-OH), 4.01 (s, 1H, H-OH), 3.77 (s, 1H, H-12), 3.59 (s, 1H, H-7), 3.16–3.11 (m, 2H, H-3, H-8), 2.21–2.12 (m, 2H,H-4a), 202–1.88 (m, 5H, H-31, H-35, H-5, H-22a, H-22b), 1.80–1.61 (m, 4H, H-25, H-1a, H-2a, H-16a), 1.64–1.57 (m, 3H, H-6a, H-2b, H-15a), 1.42–1.12 (m, 22H, H-4b, H-9, H-11a, H-11b, H-14, H-17, H-23a, H-24b, H-26a, H-29a, H-26b, H-29b, H-32a, H-32b, H-33a, H-33b, H-34a, H-34b,H-17, H-32, H-33, H-34), 0.98–0.82 (m, 8H, H-1b, H-15b, H-33b, H-34b), 0.79 (3H, s, H-19), 0.57 (3H, s, H-18); ^{13}C NMR (100 MHz, DMSO-*d$_6$*) δ_C: 35.3 (CH$_2$, C-1), 31.8 (CH$_2$, C-2), 70.4 (CH, C-3), 38.8 (CH$_2$, C-4), 41.4 (CH, C-5), 35.3 (CH$_2$, C-6), 66.2 (CH, C-7), 39.5 (CH, C-8), 28.6 (CH, C-9), 34.4 (C, C-10), 28.6 (CH$_2$, C-11), 71.0 (CH, C-12), 45.7 (C, C-13), 41.5 (CH, C-14), 22.8 (CH$_2$, C-15), 27.3 (CH$_2$, C-16), 41.5 (CH, C-17), 12.4 (CH$_3$, C-18), 22.6 (CH$_3$, C-19), 38.3 (CH, C-20),
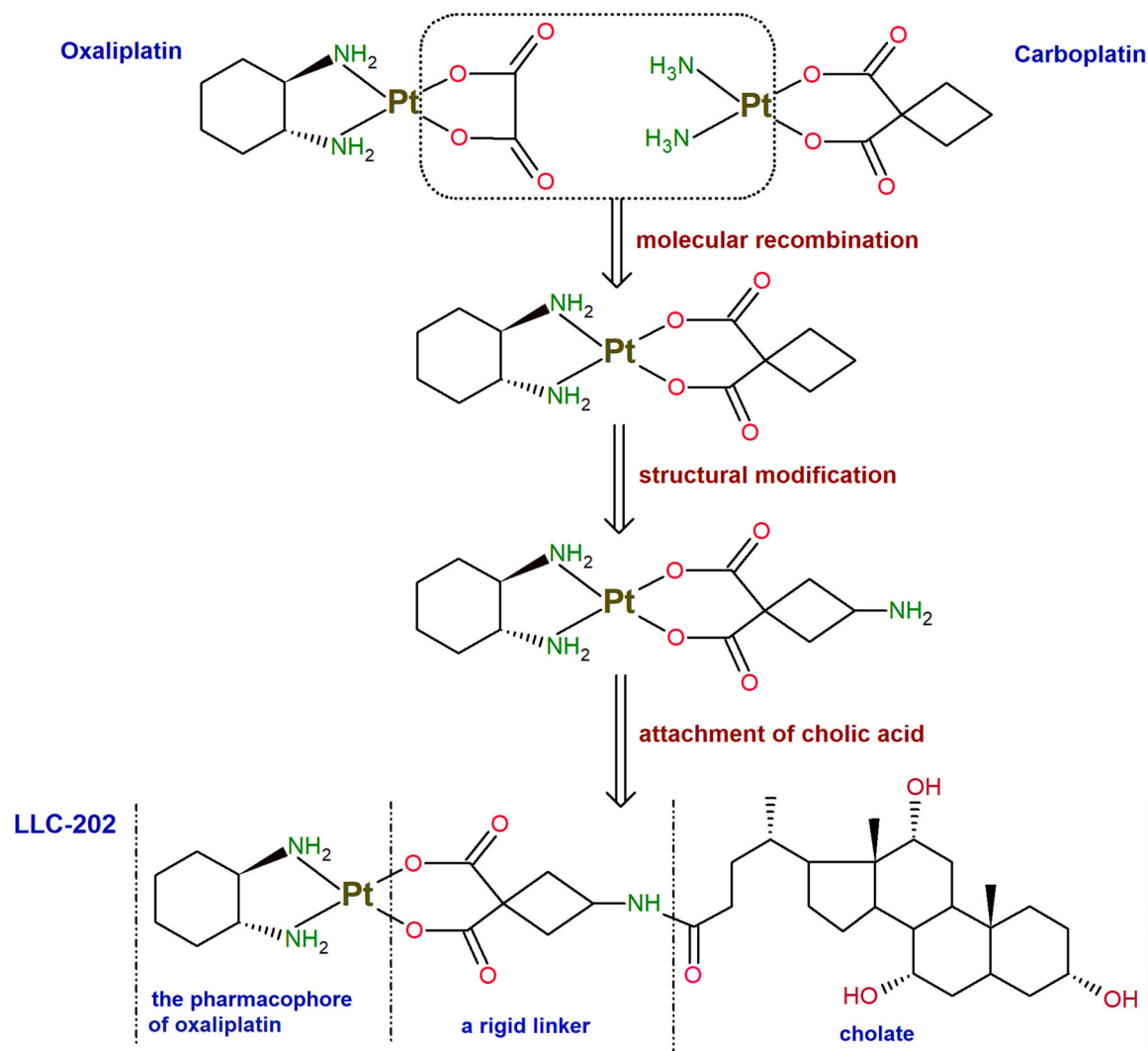
Fig. 1. Synthetic strategy of LLC-202, a prodrug of oxaliplatin. It consists of a hybrid of oxaliplatin and carboplatin, 1, 1-cyclobutane- dicarboxylic acid as the linker, and cholic acid as the liver-targeting moiety.

17.2 (CH$_3$, C-21), 32.4 (CH$_2$, C-22), 33.4 (CH$_2$, C-23), 172.0 (C, C-24), 46.1 (CH, C-25), 32.4 (CH$_2$, C-26), 50.1 (C, C-27), 176.6 (C, C-28), 31.8 (CH$_2$, C-29), 177.1 (C, C-30), 62.2 (CH, C-31), 31.5 (CH$_2$, C-32), 24.1 (CH$_2$, C-33), 24.1 (CH$_2$, C-34), 31.5 (CH$_2$, C-35), 61.9 (CH, C-36) (Fig. 2).

2.3. Physicochemical properties of LLC-202

2.3.1. Solubility

The solubility of LLC-202 in water, ethanol, olive oil, PEG-400, DMSO and DMF at room temperature were determined by the standard method of the Chinese Pharmacopoeia (CP) 2015 as follows: The test sample of LLC-202 was ground into fine powder (diameter of 0.15–0.20 mm), weighted precisely, transferred into 100 mL solvent at 25 °C ± 2 °C and shaked vigorously for 30 s every 5 min. The dissolution within 30 min was observed. If there were no visible solute particles, it was considered as complete dissolution.

2.3.2. Stability

The analytical conditions and methods of HPLC were established. Three aqueous solutions of LLC-202 (0.4 mg/mL) were placed, respectively, at 25 °C and 37 °C for 72 h or at 65 °C for 8 h. The change in the content of LLC-202 was measured by HPLC and the degradation products were identified by HPLC-MS.

2.3.3. Octanol-water partition coefficient

The distribution coefficient of LLC-202 in n-octanol-water system was also measured according to the standard method described in CP 2015.

2.4. Biological tests

The biosamples for plasma pharmacokinetics (PK) and tissue distribution studies were analyzed by DRC-e ICP-MS (PerkinElmer, USA). The analytes were injected into the ionization source by the autosampler. The main parameters of the equipment were as follows: radiofrequency power was 1.2 kW, and flow rates of cooling gas, atomizer gas, and auxiliary gas were 15 L/min, 0.7 L/min, and 1.0 L/min, respectively.

Female Sprague-Dawley (SD) rats with body weight of 200 ± 20 g were used for PK and tissue distribution studies, wild type C57BL/6 mice of both sexes with primary hepatocellular carcinoma, weighting 20 ± 2 g were used for therapeutic effect evaluation, and healthy KM mice of both sexes with body weight of 20 ± 2 g for a preliminary toxicity study. All the animals were purchased from Beijing Weitong Lihua Experimental Animal Co. Ltd., and housed in the Center of Experimental Animals of Tsinghua University, Beijing, China. All the animals were kept in a normally controlled breeding room (temperature: 20 ± 2 °C, humidity: 60 ± 5%, 12 h dark/light cycle) with standard laboratory food and water prior to the experiments. All the animals were housed with

unlimited access to food and water, except for a 24 h fast before the experiment. All animal experiments were conducted in accordance with the Institutional Animal Care and Use Committee Guidelines of Tsinghua University and the Kunming Institute of Zoology, CAS.

2.4.1. Inhibition of LLC-202 on tumor cell proliferation

The cells in a logarithmic growth stage were seeded into 96-well plates at 4000 cells per well, and cultured at 37 °C with 5% CO_2 for 24 h; then, the cells were treated with LLC-202 or oxaliplatin at different concentrations. After 72 h of drug exposure, the cell viability was measured by a methyl thiazolyl tetrazolium (MTT) assay. The inhibition rate of cell growth (%) and the half maximal inhibitory concentration (IC50) value of the compound were calculated from the dose-response curves of the assay using SPSS 24 software.

2.4.2. Therapeutic effect of LLC-202 on primary HCC in mice

Wild-type C57BL/6 mice were used as the animal model for anti-tumor tests. The primary liver cancer in the mice was induced by a one-time intra-abdominal injection of diethylnitrosamine (DEN) at a dose of 25 mg/kg when the mice were at postnatal day 15 [44], then the animals were randomly divided into 5 groups when they were 8-month-old including LLC-202 (5 mg/kg, 10 mg/kg, and 20 mg/kg), oxaliplatin (5 mg/kg), and vehicle-control group (5.9% glucose). The molar dose of 10 mg/kg for LLC-202 (12.5 μmol/kg) is the same as that of 5 mg/kg for oxaliplatin. LLC-202 was dissolved in the vehicle, an aqueous solution containing 5% glucose and 20% PEG-400, and oxaliplatin in 0.5% glucose, just before administration. Each mouse was given the corresponding dose of LLC-202, oxaliplatin or vehicle by intraperitoneal administration, once every 3 days for a total of 7 times. After administration, the survival status of the mice was observed for about 320 days. The last dead animal in each group was dissected immediately and liver tissue was taken for immunohistochemical staining (HE, Ki67, and CC3).

2.4.3. Cell uptake kinetics in vitro

LLC-202 and oxaliplatin, were dissolved in DMSO at a concentration of 2 μmol/mL for the initial solution. Normal human liver cell HL7702, human liver cancer cell HepG2 were grown at 37 °C in an environment of 5% CO_2 in Dulbecco's modified eagle medium (DMEM) and 10% fetal bovine serum (FBS). The cells were seeded into 6-well plates, 2 million per well, and placed in an incubator. After 24 h, the compound was diluted by culture medium and added to the wells at final concentration of 10 μM (DMSO concentration of 0.5%). After treatment with the compound for 15 min, 1 h, 2 h and 4 h, the cells were washed twice with phosphate buffered saline (PBS) and then collected. The content of Pt in each sample was determined by ICP-MS. The viability of cells was performed by MTT method paralleled to the experiment and the data of cell viability were used to normalize the data of Pt content.

2.4.4. PK study

LLC-202 was dissolved in a mixed solution containing 5% glucose and 20% PEG-400, and oxaliplatin in 0.5% glucose, prior to administration. Six rats were employed for the PK study of LLC-202. The rats were i.v. injected by tail vein with the drug solutions at a dose of 10.0 mg/kg body weight (2.28 mg/kg for Pt) for LLC-202. At each time point of 0.033, 0.16, 0.5, 1, 2, 4, 6, 9 and 12 h after administration, a 0.3 mL blood sample of each rat was collected from the ophthalmic venous plexus into a heparinized Eppendorf tube. The collected blood sample was centrifuged at 4 °C and 3500 rpm for 10 min, and the plasma was transferred into a clean EP tube and stored in a refrigerator at 4 °C. The PK study of oxaliplatin was performed with another 6 rats, in which a dose of 4.64 mg/kg (2.28 mg/kg for Pt) was used. All the other processes were carried out in the same way as for LLC-202.

The treatment of plasma samples was as follows: an aliquot of 0.1 mL plasma was transferred into a beaker, and 3 mL concentrated HNO_3 was added to digest the sample. The beaker was placed on a hot plate, heated and refluxed at 180 °C for 1 h till complete dissolution. After being cooled to room temperature, 0.6 mL H_2O_2 was added to the solution, and the beaker was heated on a hot plate till the sample had completely precipitated. The liquid was evaporated till 0.5 mL remained, and the residue was diluted with a 2% HNO_3 solution, and brought to a final volume of 10 mL for Pt determination.

Based on the calibration curve obtained by linear regression analysis, which was obtained with a series of standard Pt solutions of different concentrations ranging from 0 to 400 ng/mL. Duplicate measurements were detected for each sample.

All data were presented as mean ± standard deviation. PK parameters such as area under concentration–time curve (AUC), mean retention time (MRT), volume of distribution (V), Clearance (CL) and half-life ($t_{1/2}$), were calculated using DAS 2.0 software (Mathematical Pharmacology Professional Committee of China, Shanghai, China). Statistics were analyzed using Microsoft Excel 2016 (Microsoft, USA), Origin (Origin Lab, USA) and SPSS 24 (IBM, USA). Differences in indices between the LLC-202 and oxaliplatin groups were analyzed by student's t-test. A two-sided P value <0.05 was considered statistically significant.

2.4.5. Tissue distribution

Twenty-four rats were divided into 4 groups of 6 rats each, in which LLC-202 was intravenously administrated by tail veins at the same dose as in the PK study. At each time point of 0.083, 1, 4 and 8 h after administration, one group was lightly anesthetized with ether, and sacrificed by cervical spine luxation. Tissue samples including heart, liver, spleen, lung, kidney, and ovary were excised immediately and rinsed with a 0.9% saline solution, blotted with filter paper, weighed and chopped with blades, then stored at −80 °C till treatment for ICP-MS analysis. The tissue distribution of oxaliplatin was performed with another 24 rats, at the same dose as in the PK study. The tissue samples were processed in a similar way as the plasma samples, except that 2 mL concentrated HNO_3 for each 0.1 g tissue sample was used during digestion.

Based on the calibration curve obtained by linear regression analysis, which was obtained with a series of standard Pt solutions of different concentrations ranging from 0 to 400 ng/mL. Duplicate measurements
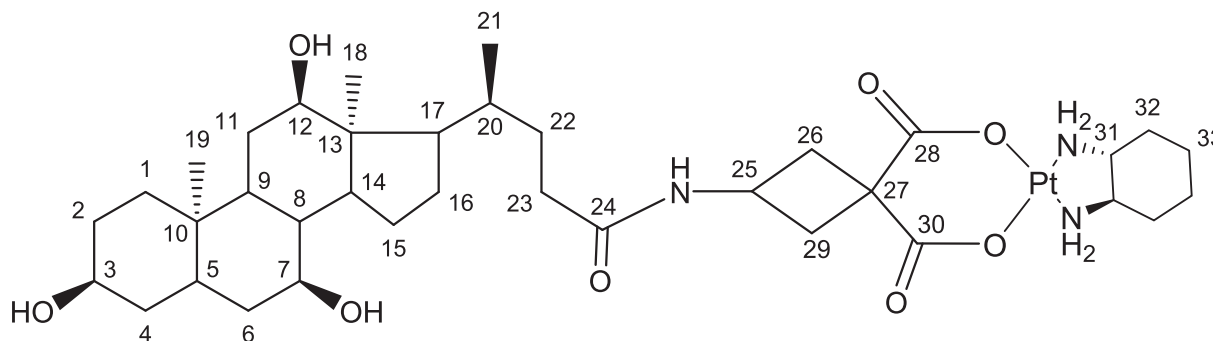

Fig. 2. Molecular structure of LLC-202.

were detected for each sample.

2.4.6. Toxicity to normal cells of the liver

Normal human liver cells HL7702 were used in this experiment. The cells in a logarithmic growth stage were seeded into 96-well plates with 4000 cells per well, and cultured at 37 °C with 5% CO$_2$ for 24 h. LLC-202 and oxaliplatin were added to the wells at a concentration of 1, 5, 10, 20, and 50 μM, and a vehicle-control group was added; all tests were performed in triplicate. After 72 h, 5 mg/mL MTT was added to each well, and the incubation was continued for 4 h. The supernatant was carefully aspirated and DMSO was added to each well. The plates were horizontally shaken for 10 min, and the light absorption value of each well was measured at 490 nm with the enzyme marker.

$$Cell\ viability\ (\%) = \frac{OD_{compound}}{OD_{solvent}} \times 100\%$$

2.4.7. Preliminary toxicity of LLC-202 to mice

Healthy KM mice of both sexes, weighting 18–22 g, were divided into 5 groups of 10 animals each, matched for weight and size. The tested drug was injected i.v. into animals, with a single dose ranging from 18 to 80 mg/kg (dissolved in 5% glucose solution containing 20% PEG-400) for LLC-202 groups and 14–31 mg/kg (dissolved in 0.5% glucose solution) for oxaliplatin groups. Dose increments confirmed to a geometric progression. Death was recorded within 14 days, and median lethal dose (LD$_{50}$) values were calculated using a Probit method. An autopsy and histopathological examination on the dead and surviving animals after the experiment were performed.

3. Results and discussion

3.1. Synthesis and characterization of LLC-202

The synthesis of LLC-202 is outlined in Schemes 1, 2 and 3, as illustrated in Fig. 3. In Schemes, 1 **1** was prepared according to our previous work [45,46] and used as the starting material. **1** was first converted to **2** in an acylation reaction with paratoluensulfonyl chloride TsCl, then to **3** by sodium azide (NaN$_3$). Reduction of N$_3^-$ with hydrogen catalyzed by Pd/C gave **4**, a compound which was finally attached to cholic acid (represented by RCOOH) via a dehydration condensation reaction between the NH$_2$ and COOH group, forming **5**. After hydrolysis of the ester bond of **5**, the desired ligand **6** for the platinum (II) center was produced. The chemical structure of **6** was confirmed by MS, ^{1}HNMR, ^{13}CNMR and 2D NMR spectra, and its purity was checked by HPLC to be >95% (Supporting Material 1).

Compound **8** was prepared using the conventional route [47] in Scheme 2. starting from a commercially available platinum compound K$_2$PtCl$_4$. K$_2$PtCl$_4$ was converted in situ to K$_2$PI$_4$, followed by addition of 1R,2R-diaminocyclohexane (A$_2$) to produce insoluble **7**. A quantitative reaction in water with silver nitrate yielded **8**.

As the water-solubility of the target compound is expected to be low, the direct reaction of *cis*-[PtA$_2$(H$_2$O)$_2$](NO$_3$)$_2$ and sodium 3-RCONH-1,1-dicarboxylate in water was used to precipitate the target compound LLC-202 (Scheme 3). LLC-202 was found to be considerably soluble in DMF despite insolubility in water. It was purified by a counter solvent recrystallization method to re-precipitate the sample for structural characterization and biological tests.

The structural characterization was performed by elemental analysis, ESI$^+$-MS and FT-IR along with ^{1}HNMR, ^{13}C NMR and 2D NMR spectra (Supporting Material 2). The data are in good agreement with the structure of LLC-202.

A Pt(IV) derivative with cholic acid directly conjugated to the axial positions of a oxaliplatin had ever been considered and tried using the synthetic method reported in the literature [43], but it could not been obtained, probably because the acidity of cholic acid is too weak to coordinate with Pt(IV) and the steric hindrance of cholic acid, a relatively large molecule, might have a negative effect on its coordination to Pt(IV).

3.2. Physicochemical properties of LLC-202

3.2.1. Solubility

LLC-202 is insoluble in water ($\approx$ 0.5 mg/mL), ethanol or olive oil ($\approx$ 1 mg/mL) but had considerable solubility in DMSO (> 5 mg/mL), DMF (> 10 mg/mL) and PEG400 ($\approx$ 9 mg/mL) at room temperature, indicating that the purification of LLC-202 could be carried out with DMF as the solvent by a counter solvent recrystallization method. PEG400 has been well known for its low toxicity and widely used as a solvent for clinical medicines [48]. Therefore, it can be used as the solvent of LLC-202 for biological experiments or manufacture of liquid preparations.

3.2.2. Octanol-water partition coefficient

The partition coefficient of LLC-202 in n-octanol-water is 0.68, which can provide an important reference for further druggability and development.

3.2.3. Stability

LLC-202 is very stable in its solid state, and the decomposition temperature is about 221 °C. It has also sufficient stability at room temperature in 0.4 mg/mL aqueous solution, and its content does not change at 25 °C and 37 °C for 72 h, as monitored by HPLC (Supporting Material 3), indicating that it can be developed as aqueous injections such as emulsions and liposomes. But as the temperature rises to 65 °C, a new chromatographic peak would develop within 8 h, which could be identified by HPLC-MS as 3-cholic amide-1,1-cyclobutane dicarboxylate. Therefore, similar to oxaliplatin, LLC-202 undergoes hydration reaction in water at high temperature, releasing the bioactive species cis-[A$_2$Pt(H$_2$O)$_2$]$^{2+}$ (required for the anticancer activity) and 3-cholic amide-1,1-cyclobutane dicarboxylate, as shown in Fig. 4. However, under the experimental conditions, no amide bond hydrolysis products were detected, suggesting that the coupling of cholic acid with the used linker should relatively stable to resist hydrolysis.

3.3. In vitro and in vivo anticancer activity of LLC-202

#### 3.3.1. In vitro anticancer activity of LLC-202

The in vitro anticancer activity of LLC-202 was compared with that of oxaliplatin in human liver carcinoma cell line HepG2. Cell viability was determined by means of the MTT protocol after 72 h of drug treatment, and the results are given in Fig. 5. It is interesting that for HepG2, LLC-202 shows a bit higher activity with lower IC50 values compared with oxaliplatin. It is possibly caused by the bile acid receptors located in the cell membrane of liver carcinoma cells which leads to a higher uptake of LLC-202. For further research in future, it is necessary to reinforce the mechanisms of LLC-202 in cells after its uptake by liver cancer cells.

#### 3.3.2. Therapeutic effect of LLC-202 on primary HCC in mice

The survival curves of C57BL/6 mice with primary hepatocellular carcinoma are shown in Fig. 6. For the vehicle-control group, only 68%, 29%, 6%, and 0% mice survived after 100, 150, 250, and 300 days, respectively. Following i.v. administration of oxaliplatin at a dose of 5 mg/kg, the survival rates were significantly improved at 92%, 53%,
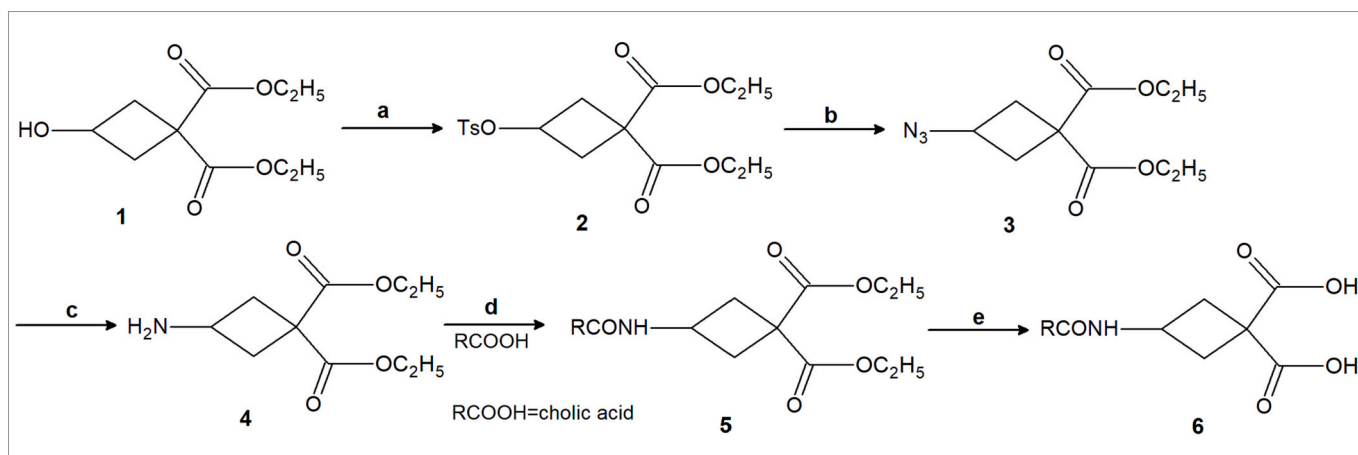
Scheme 1. a) TsCl, Et$_3$N, DMAP, DCM, 0 °C-room temperature; b) NaN$_3$, Bu$_4$NHSO$_4$, DMF, 80 °C; c) Pd/C, H$_2$; d) DCC, HOBt, NMM, −15 °C; e) NaOH, MeOH, 50 °C.
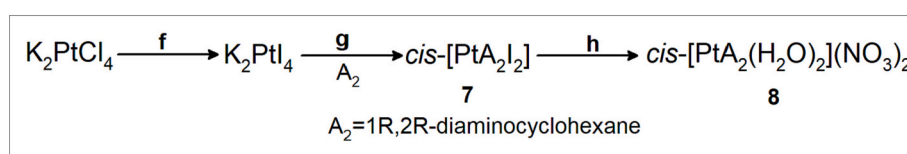
Scheme 2. f) KI, at room temperature, 4 h; g) at room temperature, 2 h; h) AgNO$_3$, at 45 °C, 24 h
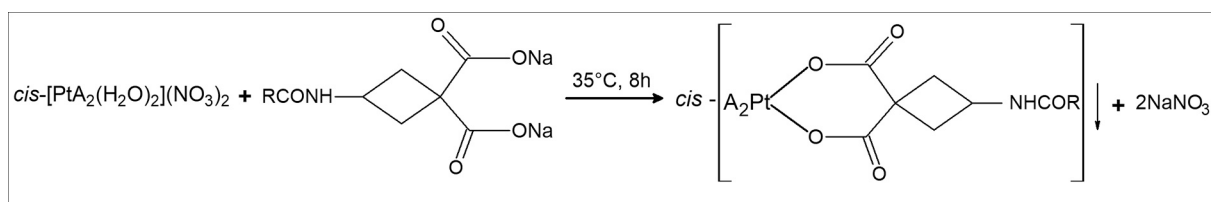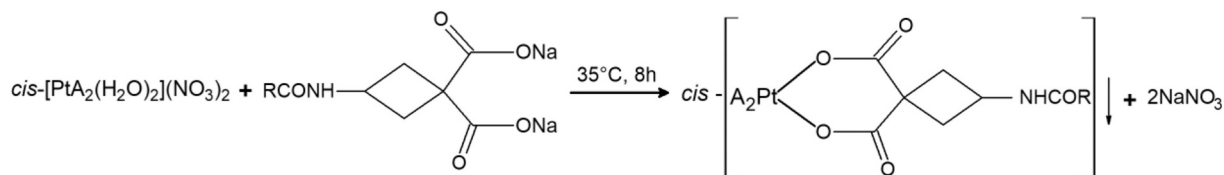

Scheme 3.

Fig. 3. Synthesis routes and conditions of LLC-202.

23%, and 23%, correspondingly ($P < 0.05$). For the group treated with a low dose of LLC-202 (5 mg/kg), the survival rates of mice were 69%, 61%, 31%, and 15%, indicating that this dose was relatively low, and some mice died for the cancer. For the group with a high dose of LLC-202 (20 mg/kg), the survival rates were 68%, 50%, 38%, and 31%, which was also relatively low, and should be caused by the toxicity of LLC-202. However, for the group with the middle dose of LLC-202 (10 mg/kg), the survival rates were 92%, 77%, 61%, and 53%, significantly higher than the oxaliplatin group ($P < 0.05$) and the vehicle-control group ($P < 0.01$), showing that 10 mg/kg was the best of the tested doses, and had a significant inhibitory effect on primary hepatic cancer in mice.

The immunohistochemical staining of mouse liver tissue in each group is shown in Fig. 7. Hematoxylin-eosin staining (HE) was used to identify tumor tissues. Compared to vehicle-control group (5.9% glucose) and oxaliplatin group (5 mg/kg), the number of Ki67-positive cells (the number of brown dots and the depth of color) was significantly decreased in the LLC-202 medium-dose group (10 mg/kg), but the number of cleaved-caspase3 (CC3) was significantly increased, indicating that there was a large amount of apoptosis in tumor cells and that the malignant degree of HCC could be significantly lowered after administration of LLC-202 at a dose of 10 mg/kg.

3.4. Cell uptake kinetics in vitro and pharmacokinetic investigation in rats

3.4.1. Cell uptake kinetics in vitro

After culturing with LLC-202 and oxaliplatin at a final concentration of 10 μM for 15 min, 1 h, 2 h and 4 h, the two human cell lines including one normal liver cell line and one liver cancer cell line were washed twice with PBS and collected. The content of Pt in each sample was determined by ICP-MS. The total Pt uptake of each compound by the cells is given in Fig. 8, which indicates that the normal human liver cell line HL7702 has a relatively low uptake of LLC-202, compared with the prototype drug oxaliplatin ($p < 0.05$ at 4 h). On the contrary, human liver cancer cell line HepG2 displays significantly higher uptake of LLC-202 compared with oxaliplatin ($p < 0.05$, $p < 0.01$). It is interesting that significant higher uptake by HepG2 cells of LLC-202 compared to oxaliplatin is observed even at 15 min, indicating that HepG2 cells may be more sensitive to this cholic modified prodrug than to oxaliplatin.

As mentioned in the introduction, it has been known that there are various bile acid receptors such as GPBAR, TGR5, FXR, SLC10A1, and NTCP, etc., that located in cell membrane or nucleus and the function and transport mechanisms of these receptors are very complicated and not completely clear so far. It is a pity that there has been no literature directly reporting the expression difference of cholic acid between HepG2 and HL7702. The research showed that FXR had a lower expression in HCC tissue compared with norm liver tissue [49] which seems not to support our result, but it was also reported that the high ratio of FXRα1/FXRα2 could lead to HCC [50], meaning the expression ration of receptors is important which can possibly support our result more or less. These researches also reflect the complication and diversification of bile acid receptors and further research should be performed in future.

3.4.2. PK study

All the rats were intravenously injected through their tail vein with the same Pt dose at 2.28 mg/kg body weight. The PK concentration–time profiles of Pt for oxaliplatin and LLC-202 are shown in Fig. 9. According to the analysis by the DAS 2.0 software, the metabolic process in vivo conformed with a two-compartment open model which meant that the distribution and balance speed of drugs in plasma and tissues were different, which coul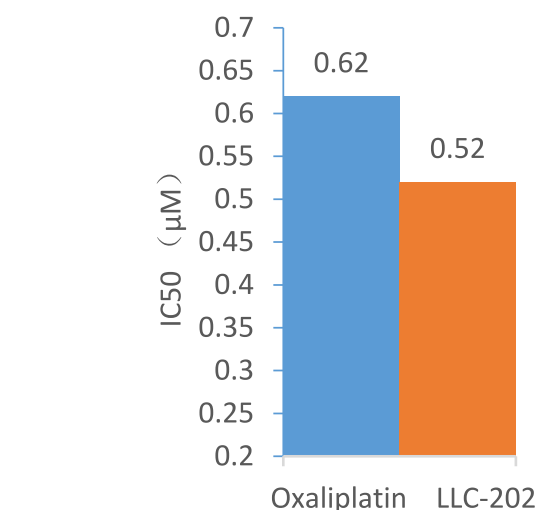d be divided into central chamber (including blood and tissues with rich blood flow such as liver and kidney) and peripheral chamber (tissues with poor blood flow such as fat and bone), and drugs entered the central chamber first and distributed instantaneously and evenly in this chamber, then slowly distributed to the peripheral chamber. The major PK parameters of Pt for oxaliplatin and LLC-202 are shown in Table 2. The concentrations of Pt for LLC-202 at all time-points were much higher than those for oxaliplatin. Most parameters of Pt for LLC-202 showed a statistically significant difference from those for oxaliplatin.

The area under the curve (AUC) data of Pt for LLC-202 (AUC_{0-t} 35.23 $\pm$ 6.17 mg/L·h and $AUC_{0-\infty}$ 41.94 $\pm$ 6.91 mg/L·h) far exceed those for oxaliplatin (AUC_{0-t} 7.91 $\pm$ 0.64 mg/L·h and $AUC_{0-\infty}$ 11.03 $\pm$ 0.71 mg/L·h) ($P < 0.01$), indicating that the plasma exposure of LLC-202 was significantly higher than oxaliplatin. Both clearance (CL) and apparent volume of distribution (Vd) data of Pt for LLC-202 were significantly lower than those for oxaliplatin ($P < 0.01$), which strongly supports the higher AUC of Pt for LLC-202 compared to oxaliplatin. Therefore, the
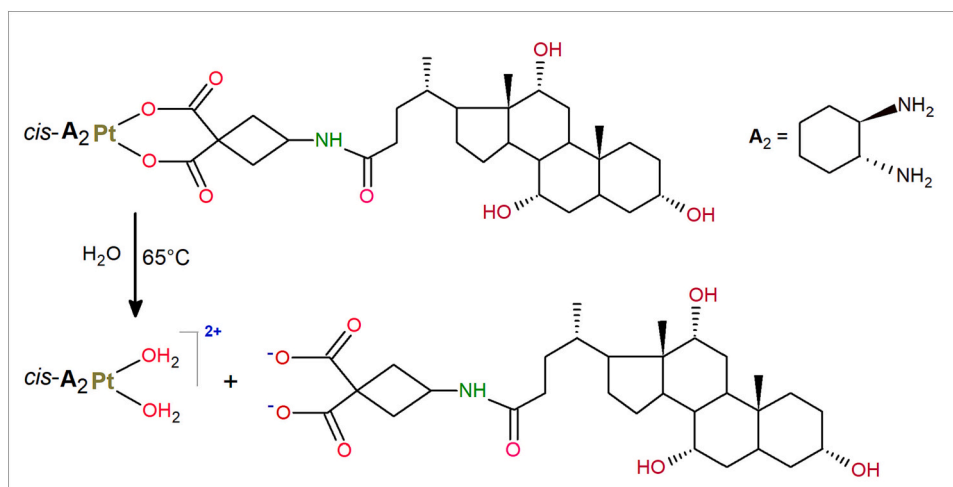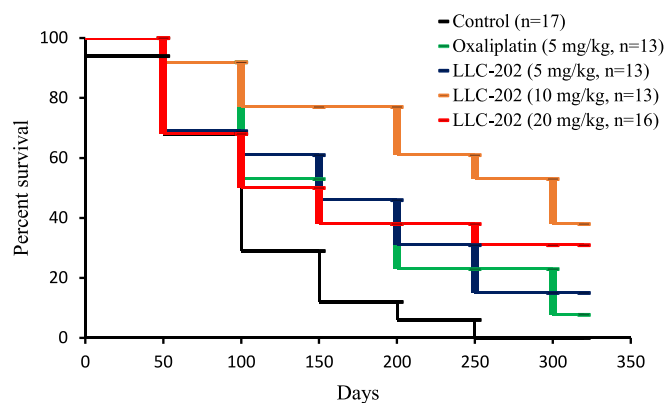

Fig. 5. In vitro anticancer activity of LLC-202 against HepG2 (IC $_{50}$, μM, $n = 3$, SD $\leq 15\%$).

Fig. 4. Hydration reaction of LLC-202 in aqueous solution.

Control vs oxaliplatin (5 mg/kg): p=0.041

Control vs LLC -202 (10 mg/kg): p<0.01

Fig. 6. Survival curves of mice with primary hepatocellular carcinoma after administration of LLC-202 and oxaliplatin, showing that 10 mg/kg of LLC-202 is the best dose and has a significant inhibitory effect on primary hepatic cancer in mice.

superiority of LLC-202 in antitumor activity over oxaliplatin is probably due to its greater hydrophobicity compared to oxaliplatin. Based on the calculation by statistical moment method, the mean retention time ($MRT_{0-\infty}$) of LLC-202 (5.14 ± 0.43 h) was significantly lower than that of oxaliplatin (9.89 ± 2.29 h) ($P < 0.01$), similar to the tendency of elimination half-life ($t_{1/2\beta}$) data (4.34 ± 0.8 h for LLC-202 and 6.22 ± 2.21 h for oxaliplatin, but $p > 0.05$).

3.4.3. Tissue distribution

The tissue distribution of Pt for oxaliplatin and LLC-202 at 4 different time points (5 min, 1 h, 4 h, and 8 h) is shown in Fig. 10. In heart, Pt concentration for LLC-202 was significantly different from oxaliplatin at

any time point ($p < 0.05$, $p < 0.01$). Pt concentration for LLC-202 at 0.083 h was higher than that for oxaliplatin ($p < 0.01$), while lower at 1, 4, and 8 h ($p < 0.05$, $p < 0.01$, $p < 0.01$). In liver and spleen, Pt concentration for LLC-202 was significantly higher than oxaliplatin at any time point ($p < 0.05$, $p < 0.01$). In lung, Pt concentration for LLC-202 was significantly higher at 0.083 h and 1 h ($p < 0.01$), lower at 8 h ($p < 0.05$) and there was no significant difference at 4 h. In kidney, Pt concentration for LLC-202 was lower than that for oxaliplatin at 0.083 h and 8 h ($p < 0.01$, $p < 0.05$). In ovary, there was no significant difference of Pt concentration between LLC-202 and oxaliplatin at any time point ($p > 0.05$).

It could also be found that for oxaliplatin, Pt concentration at each time point was the highest in kidney and the lowest in heart, compared with the other tissues. For LLC-202, Pt concentration was the highest in liver and the lowest in heart at each time point. The concentration in liver was 2–3 times higher than those in the other tissues. The levels of Pt in spleen, lung, kidney, and ovary were different at each time point for either oxaliplatin or LLC-202.

The $AUC_{5min-8h}$ data of Pt for oxaliplatin and LLC-202 are shown in Fig. 11. For the tissue distribution of oxaliplatin, the $AUC_{5min-8h}$ of Pt in kidney was the largest, probably due to its renal elimination, while for LLC-202 the $AUC_{5min-8h}$ of Pt in liver was the largest. The concentrations of Pt for LLC-202 in liver, spleen and lung are significantly higher compared with oxaliplatin, while the concentrations in heart and kidney are lower and there was no significant difference in ovary ($p > 0.05$).

According to the comparison above, it could be concluded that LLC-202 was mainly distributed in the liver after administration, significantly different from oxaliplatin which is localized mainly in the kidney, showing a notable liver-targeted effect of LLC-202 based on its modification with cholic acid. It was also very interesting that LLC-202 had high distribution at 0.083 h after administration. It should be emphasized that some lung cancer cells also had high bile acid receptors, which could be the new potential application of LLC-202. For example, Farnesoid X receptor (FXR) is a bile acid receptor encoded by the Nr1h4 gene. In recent years, several studies have shown that FXR is widely involved in the pathogenesis of various respiratory diseases, such as
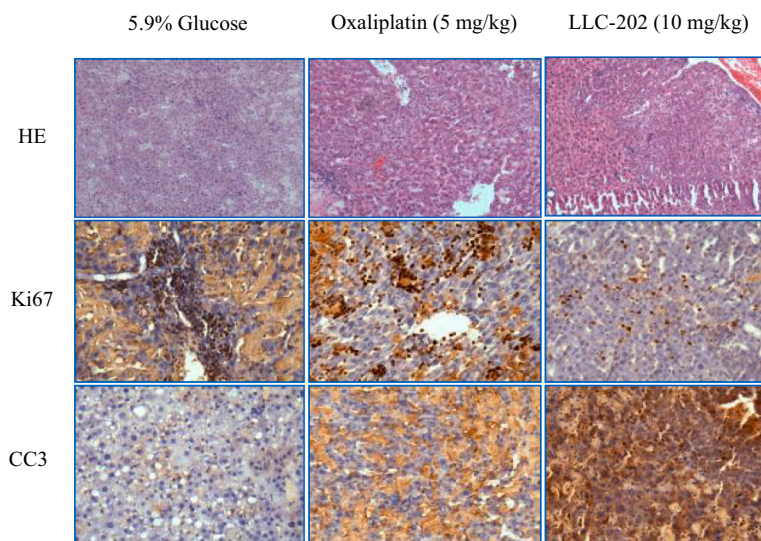

Fig. 7. Immunohistochemical staining of mouse liver tissue after administration of 5.9% glucose (vehicle-control group), oxaliplatin (5 mg/kg) or LLC-202 (10 mg/kg). The result indicates that there is a large amount of apoptosis in tumor cells and that the malignant degree of HCC can be significantly lowered after administration of LLC-202.
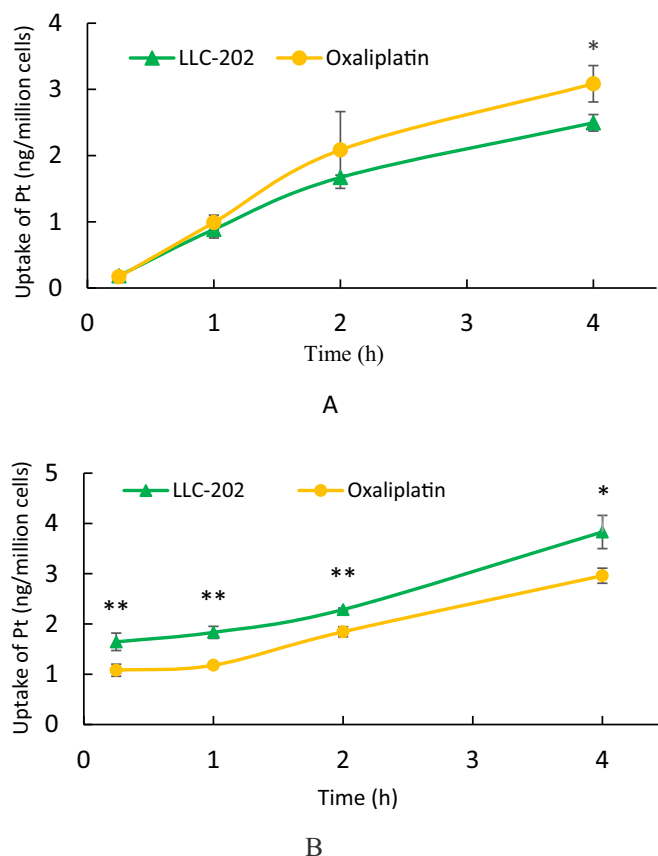
Fig. 8. Uptake of Pt in LLC-202 and oxaliplatin by normal human liver cell HL7702 (A) and human liver cancer cell HepG2 (B), indicates that LLC-202 can be more easily transferred into liver cancer cells and has less uptake by normal human liver cell compared with oxaliplatin (t-test, * $p < 0.05$; ** $p < 0.01$).
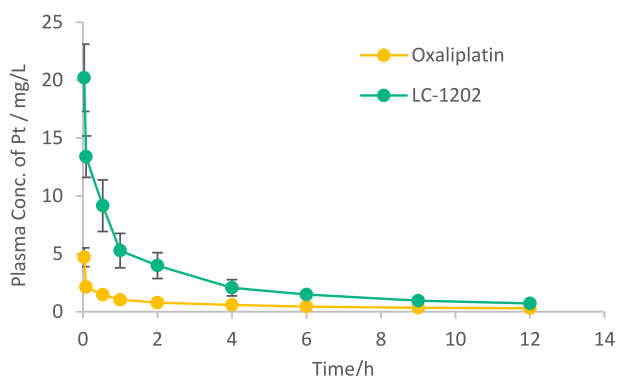

Fig. 9. Plasma concentration-time profiles of Pt of oxaliplatin and LLC-202 after i.v. administration to rats with a single dose of 2.28 mg/kg calculated by Pt ($n = 6$).

chronic obstructive pulmonary disease, bronchial asthma, and idiopathic pulmonary fibrosis. Moreover, a number of works have confirmed that FXR can regulate the bile acid metabolism in the body and exert its

Table 2

PK parameters of Pt of LLC-202 and oxaliplatin in plasma after i.v. administration to rats with a single dose of 2.28 mg/kg calculated by Pt (Mean $\pm$ SD, n = 6).

Parameters	Oxaliplatin	LLC-202
$t_{1/2\alpha}$ (h)	0.14 ± 0.06	$0.34 \pm 0.13**$
$t_{1/2\beta}$ (h)	6.22 ± 2.21	4.34 ± 0.86
Vd_1 (L/kg)	0.43 ± 0.07	$0.11 \pm 0.02**$
Vd_2 (L/kg)	1.41 ± 0.32	$0.20 \pm 0.06**$
CL_1 (L/h/kg)	0.23 ± 0.04	$0.06 \pm 0.01**$
CL_2 (L/h/kg)	1.66 ± 0.55	$0.12 \pm 0.05**$
AUC_{0-t} (mg/L·h)	7.91 ± 0.64	$35.23 \pm 6.17**$
$AUC_{0-\infty}$ (mg/L·h)	11.03 ± 0.71	$41.94 \pm 6.91**$
K_{10} (1/h)	0.55 ± 0.14	0.60 ± 0.10
K_{12} (1/h)	4.04 ± 1.77	$1.18 \pm 0.60**$
K_{21} (1/h)	1.26 ± 0.54	0.67 ± 0.37
MRT_{0-t} (h)	3.96 ± 0.18	$3.01 \pm 0.18**$
$MRT_{0-\infty}$ (h)	9.89 ± 2.29	$5.14 \pm 0.43**$

**t-test, $p < 0.01$ compared to the data of oxaliplatin.

anti-inflammatory and antifibrotic effects in the airways and lungs [51].

3.5. Toxicity investigation

3.5.1. Toxicity to normal liver cells

The cell viability (%) of normal human liver cells HL7702 is shown in Fig. 12 after treatment for 72 h with different concentrations of LLC-202 and oxaliplatin, respectively. With the increase of the concentration of oxaliplatin or LLC-202, the survival of cells decreased, indicating that the toxicity increased. Compared with oxaliplatin, LLC-202 was less toxic to HL7702 cells at each concentration ($p < 0.05$, $p < 0.01$) which might be caused by lower uptake of LLC-202 by HL7702 than that of oxaliplatin. At the high concentration of 100 μM the cell viability was similar (p < 0.01). By SPSS 24 software, the IC_{50} values of LLC-202 and oxaliplatin were estimated 16.029 μM(13.73 mg/L) and 5.354 μM(2.13 mg/L), respectively.

3.5.2. Preliminary toxicity for mice

Within 24 h after administration of LLC-202 and oxaliplatin, the mice in each group showed different degrees of hypophagia, hypo-activity, mental aberration, hair bristling and death. Death mainly took place during the 3rd ~ 6th day after administration. The food uptake and motor activity increased and the activity was gradually recovered after 7 days.

The LD_{50} of LLC-202 and oxaliplatin was 43.0 mg/kg (50.2 μmol/kg) and 20.0 mg/kg (50.3 μmol/kg), respectively, showing similar acute toxicity of LLC-202 and oxaliplatin in molar terms. Histopathological examination (Table 3, Supporting Material 4) showed that the bone marrow hematopoietic cells of each line in the LLC-202 dose groups were slightly to severely decreased, and there was an obvious dose-response relationship. The incidence and lesion degree of the low-dose group and the medium-dose group were less than the oxaliplatin dose group, and no pathological changes of the kidney and lung tissues were caused. In the LLC-202 high-dose group (about 2 times the LD_{50} and 1.3 times the high dose of oxaliplatin in molarity), 4 cases of diffuse liver sinus dilatation and congestion were observed, and no similar lesions were observed in the oxaliplatin group, suggesting hepatotoxicity of high-dose LLC-202. There was also some small focal inflammation in the liver, but these were spontaneous histopathological changes, and not caused by drug administration; they are commonly observed in mice.
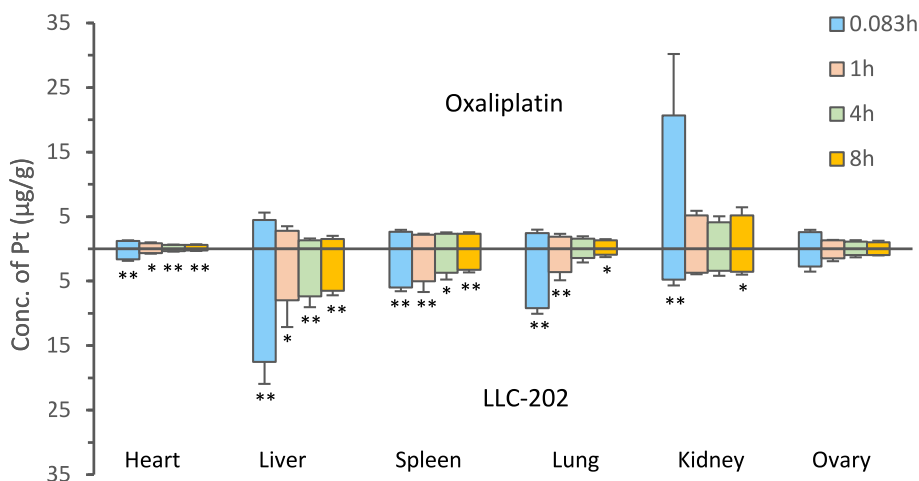
Fig. 10. Tissue distribution of Pt for LLC-202 and oxaliplatin after i.v. administration to rats at a single dose of 2.28 mg/kg calculated by Pt ($n = 6$) (t-test, * $p < 0.05$, ** $p < 0.01$), shows that LLC-202 is mainly distributed in liver after i.v. administration compared with oxaliplatin.
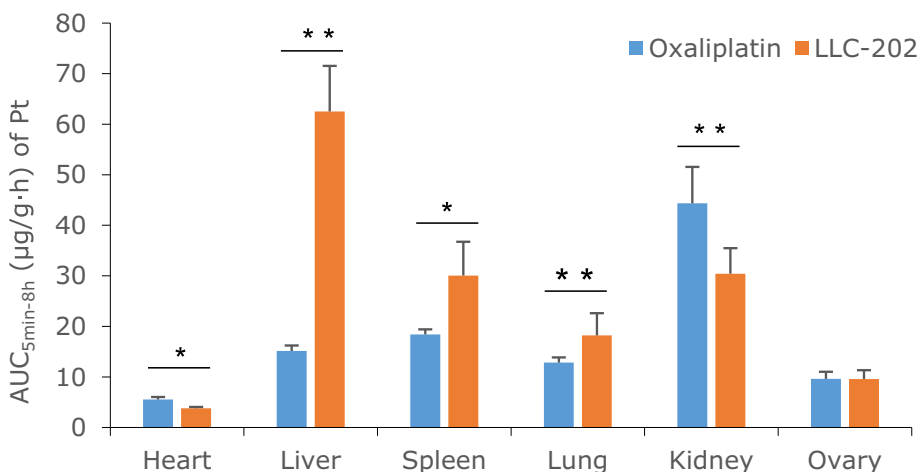

Fig. 11. $AUC_{5min-8h}$ (μg/g·h) of Pt of LLC-202 and oxaliplatin in tissue after *i.v.* administration to rats with a single dose of 2.28 mg/kg Pt (Mean ± SD, n = 6) (t-test, * p < 0.05, ** p < 0.01, compared to the data of oxaliplatin).
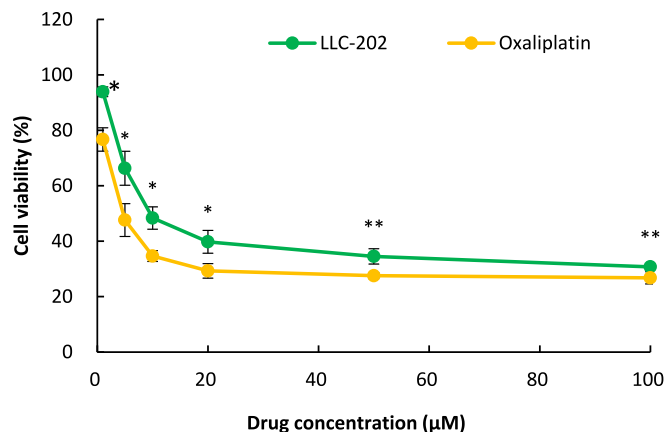

Fig. 12. Cell viability (%) of HL7702 cells after treatment with different concentrations of oxaliplatin and LLC-202 for 72 h. Compared with oxaliplatin, LLC-202 is less toxic to HL7702 cells at each concentration (* p < 0.05, ** p < 0.01).

4. Conclusions

In this paper, we have presented a novel oxaliplatin prodrug LLC-202 specific for liver cancer, based on the conjugation with cholic acid as a targeting carrier for delivering oxaliplatin to the liver, with an aim to improve its anti-tumor potency and reduce side-effects. The synthesis of LLC-202 can be accomplished at a batch quantity scale by a limited number of reaction steps under mild reacting conditions, and its physicochemical properties are acceptable from a druggability point of view. LLC-202 did show superior anticancer profile over oxaliplatin in cell and animal models. PK and tissue distribution showed that LLC-202 was mainly distributed in the liver after i.v. administration, significantly different from oxaliplatin which was found mainly in kidney, showing a significant liver-targeted effect of LLC-202. Our present studies suggest that LLC-202 is worthy of further evaluation and development as a new drug candidate for liver cancer.

Author contributions

J.J, F. H., and K. C contributed equally to this work. Q.S. and C·Y contributed to animal experiment. A.G and J.Y contributed to synthesis.

Table 3
Histopathological changes following administration of LLC-202 and oxaliplatin to mice.

Organ	Pathological changes	Semi-quantitative classification	Oxaliplatin			LLC-202		
			18.6 mg/kg	24.0 mg/kg	31.0 mg/kg	25.3 mg/kg	45.0 mg/kg	80.0 mg/kg
			(n = 4)	(n = 4)	(n = 4)	(n = 4)	(n = 4)	(n = 4)
Sternum	Decreased hematopoietic cells in the bone marrow	+	4	4	0	0	0	0
		++	0	0	0	0	1	0
		+++	0	0	4	0	0	4
Liver	The liver sinus dilates and extravasates blood	+	0	0	0	0	0	0
		++	0	0	0	0	0	4

() is the total number of animals. "+" represents mild or small lesions, "++" represents moderate or moderate lesions, "+++" represents severe or multiple lesions.

X.F and Y.H. contributed to cell experiments and PK investigation. W.L. contributed to design, supervision and synthesis. Y.S. and Q.L. contributed to design, supervision, writing draft, and editing.

Declaration of Competing Interest

We declare that we have no financial and personal relationships with other people or organizations that can inappropriately influence our work, there is no professional or other personal interest of any nature or kind in any product, service and/or company that could be construed as influencing the position presented in, or the review of, the manuscript.

Data availability

Data will be made available on request.

Acknowledgements

Appendix A. Supplementary data

Supplementary data to this article can be found online at https://doi.org/10.1016/j.jinorgbio.2023.112200.

References

[1] R.L. Siegel, K.D. Miller, A. Jemal, Cancer statistics, CA Cancer J. Clin. 70 (2020) 7–30.
[2] W. Chen, R. Zheng, P.D. Baade, S. Zhang, H. Zeng, F. Bray, A. Jemal, X.Q. Yu, J. He, Cancer statistics in China, CA Cancer J. Clin. 66 (2016) 115–132.
[3] E.U. Cidon, Systemic treatment of hepatocellular carcinoma: past, present and future, World J. Hepatol. 9 (2017) 797–807.
[4] A. Vogel, A. Cervantes, I. Chau, B. Daniele, J.M. Llovet, T. Meyer, J.C. Nault, U. Neumann, J. Ricke, B. Sangro, P. Schirmacher, C. Verslype, C.J. Zech, D. Arnold, E. Martinelli, Hepatocellular carcinoma: ESMO clinical practice guidelines for diagnosis, treatment and follow-up, Ann. Oncol. 29 (2018) 238–255.
[5] Bureau of Medical Administration, National Health Commission of the People's Republic of China, Guidelines for diagnosis and treatment of primary liver cancer in China (2019 Edition), J. Clin. Hepatol. 36 (2020) 277–292 (in Chinese).
[6] S.K. Qin, Y. Cheng, J. Liang, L. Shen, Y.X. Bai, J.F. Li, J. Fan, L.A. Liang, Y.Q. Zhang, G. Wu, Efficacy and safety of the FOLFOX4 regimen versus doxorubicin in Chinese patients with advanced hepatocellular carcinoma: a subgroup analysis of the EACH study, Oncologist. 19 (2014) 1169–1178.
[7] L. Kelland, The resurgence of platinum-based cancer chemotherapy, Nat. Rev. Cancer 7 (2007) 573–584.
[8] J. Graham, M. Mushin, P. Kirkpatrick, Oxaliplatin, Nat. Rev. Drug Discov. 3 (2004) 11–12.
[9] S. Qin, Y. Bai, H.Y. Lim, S. Thongprasert, Y. Chao, J. Fan, T. Yang, V. Bhudhisawasdi, W.K. Kang, Y. Zhou, J.H. Lee, Y. Sun, Randomized, multicenter, open-label study of oxaliplatin plus fluorouracil/leucovorin versus doxorubicin as palliative chemotherapy in patients with advanced hepatocellular carcinoma from Asia, J. Clin. Oncol. 31 (2013) 3509–3517.
[10] B. Liao, Y. Zhang, Q. Sun, P. Jiang, Vorinostat enhances the anticancer effect of oxaliplatin on hepatocellular carcinoma cells, Cancer Med. 7 (2018) 196–207.
[11] Y. Ma, M. Zhang, J. Wang, X. Huang, X. Kuai, Y. Chen, L. Jia, Z. Feng, Q. Tang, Z. Liu, High-affinity human anti-c-Met IgG conjugated to oxaliplatin as targeted chemotherapy for hepatocellular carcinoma, Front. Oncol. 9 (2019) 717.
[12] C.A. Rabik, M.E. Dolan, Molecular mechanisms of resistance and toxicity associated with platinating agents, Cancer Treat. Rev. 33 (2007) 9–23.
[13] W. Kramer, G. Wess, Bile acid transport systems as pharmaceutical targets, Eur. J. Clin. Investig. 26 (1996) 715–732.
[14] W. Kramer, G. Wess, G. Schubert, M. Bickel, F. Girbig, U. Gutjahr, S. Kowalewski, K.H. Baringhaus, A. Enhsen, H. Glombik, A. Et, Liver-specific drug targeting by coupling to bile acids, J. Biol. Chem. 267 (1992) 18598–18604.
[15] D.K. Meijer, Drug targeting to the liver with bile acids: the "Trojan horse" resurrected? Hepatology. 17 (1993) 945–948.
[16] M.J. Monte, S. Dominguez, M.F. Palomero, R.I. Macias, J.J. Marin, Further evidence of the usefulness of bile acids as molecules for shuttling cytostatic drugs toward liver tumors, J. Hepatol. 31 (1999) 521–528.
[17] S. Qian, J.B. Wu, X.C. Wu, J. Li, Y. Wu, Synthesis and characterization of new liver targeting 5-fluorouracil-cholic acid conjugates, Arch. Pharm (Weinheim). 342 (2009) 513–520.
[18] M.F. Dominguez, R.I. Macias, I. Izco-Basurko, A. de La Fuente, M.J. Pascual, J.M. Criado, M.J. Monte, J. Yajeya, J.J. Marin, Low in vivo toxicity of a novel cisplatin-ursodeoxycholic derivative (Bamet-UD2) with enhanced cytostatic activity versus liver tumors, J. Pharmacol. Exp. Ther. 297 (2001) 1106–1112.
[19] A. Zimber, C. Gespach, Bile acids and derivatives, their nuclear receptors FXR, PXR and ligands: role in health and disease and their therapeutic potential, Anti Cancer Agents Med. Chem. 8 (2008) 540–563.
[20] F.G. Schaap, M. Trauner, P.L. Jansen, Bile acid receptors as targets for drug development, Nat. Rev. Gastroenterol. Hepatol. 11 (2014) 55–67.
[21] D.Q. Chen, X. Wang, L. Chen, J.X. He, Z.H. Miao, J.K. Shen, Novel liver-specific cholic acid-cytarabine conjugates with potent antitumor activities: synthesis and biological characterization, Acta Pharmacol. Sin. 32 (2011) 664–672.
[22] J.J. Criado, M.C. Herrera, M.F. Palomero, M. Medarde, E. Rodriguez, J.J. Marin, Synthesis and characterization of a new bile acid and platinum (II) complex with cytostatic activity, J. Lipid Res. 38 (1997) 1022–1032.
[23] J.J. Marin, M.C. Herrera, M.F. Palomero, R.I. Macias, M.J. Monte, M.Y. El-Mir, G.R. Villanueva, Rat liver transport and biotransformation of a cytostatic complex of bis-cholylglycinate and platinum (II), J. Hepatol. 28 (1998) 417–425.
[24] M.C. Martinez-Diez, M.G. Larena, M.A. Serrano, R.I. Macias, I. Izco-Basurko, J.J. Marin, Relationship between DNA-reactivity and cytostatic effect of two novel bile acid-platinum derivatives, Bamet-UD2 and Bamet-D3, Anticancer Res. 20 (2000) 3315–3321.
[25] O. Briz, M.A. Serrano, N. Rebollo, B. Hagenbuch, P.J. Meier, H. Koepsell, J.J. Marin, Carriers involved in targeting the cytostatic bile acid-cisplatin derivatives cis-diammine-chloro-cholylglycinate-platinum (II) and cis-diammine-bisursodeoxycholate-platinum (II) toward liver cells, Mol. Pharmacol. 61 (2002) 853–860.
[26] B. Seroka, Z. Łotowski, A. Wojtkielewicz, P. Bazydło, E. Dudź, A. Hryniewicka, J.W. Morzycki, Synthesis of steroidal 1,2- and 1,3-diamines as ligands for transition metal ion complexation, Steroids. 147 (2019) 19–27.
[27] R. Paschke, J. Kalbitz, C. Paetz, Novel spacer linked bile acid-cisplatin compounds as a model for specific drug delivery, synthesis, and characterization, Inorg. Chim. Acta 304 (2000) 241–249.
[28] R. Paschke, J. Kalbitz, C. Paetz, M. Luckner, T. Mueller, H.J. Schmoll, H. Mueller, E. Sorkau, E. Sinn, Cholic acid-carboplatin compounds (CarboChAPt) as models for specific drug delivery: synthesis of novel carboplatin analogous derivatives and comparison of the cytotoxic properties with corresponding cisplatin compounds, J. Inorg. Biochem. 94 (2003) 335–342.
[29] J.J. Criado, M.F. Domínguez, M. Medarde, E.R. Fernández, R.I. Macías, J. Marín, Structural characterization, kinetic studies, and in vitro biological activity of new cis-diamminebis-cholylglycinate (O, O′) Pt (II) and cis-diamminebis-ursodeoxycholate (O, O′) Pt (II) complexes, Bioconjug. Chem. 11 (2000) 167–174.

[30] J.J. Criado, R.I.R. Macias, M.J. Medarde, M.A. Monte, J.J.G. Serrano, M. Marin, Synthesis and characterization of the new cytostatic complex cis-diammineplatinum(II) chlorocholylglycinate, Bioconjug. Chem. 8 (1997) 453–458.

[31] T.C. Johnstone, K. Suntharalingam, S.J. Lippard, The next generation of platinum drugs: targeted Pt(II) agents, nanoparticle delivery, and Pt(IV) prodrugs, Chem. Rev. 116 (2016) 3436–3486.

[32] E. Lozano, M.J. Monte, O. Briz, A. Hernandez-Hernandez, J.M. Banales, J.J. Marin, R.I.R. Macias, Enhanced antitumour drug delivery to cholangiocarcinoma through the apical sodium-dependent bile acid transporter (ASBT), J. Control. Release 216 (2015) 93–102.

[33] B. Seroka, Z. Łotowski, A. Hryniewicka, L. Rárová, R.R. Sicinski, A.M. Tomkiel, J. W. Morzycki, Synthesis of new cisplatin derivatives from bile acids, Molecules. 25 (2020) 655–670.

[34] Y. Huang, E. Kong, C. Gan, Z. Liu, Q. Lin, J. Cui, Synthesis and antiproliferative activity of steroidal thiosemicarbazone platinum (Pt (II)) complexes, Bioinorg. Chem. Appl. 2015 (2015) 1–7.

[35] L. Fang, M. Feng, F. Chen, X. Liu, H. Shen, J. Zhao, S. Gou, Oleanolic acid-NO donor-platinum (II) trihybrid molecules: targeting cytotoxicity on hepatoma cells with combined action mode and good safety, Bioorg. Med. Chem. 24 (2016) 4611–4619.

[36] F. Yang, C. Mao, L. Guo, J. Lin, Q. Ming, P. Xiao, X. Wu, Q. Shen, S. Guo, D.D. Shen, R. Lu, L. Zhang, S. Huang, Y. Ping, C. Zhang, C. Ma, K. Zhang, X. Liang, Y. Shen, F. Nan, F. Yi, V.C. Luca, J. Zhou, C. Jiang, J.P. Sun, X. Xie, X. Yu, Y. Zhang, Structural basis of GPBAR activation and bile acid recognition, Nature. 587 (2020) 499–504.

[37] F. Yang, C. Mao, L. Guo, J. Lin, Q. Ming, P. Xiao, X. Wu, Q. Shen, S. Guo, D. Shen, R. Lu, L. Zhang, S. Huang, Y. Ping, C. Zhang, C. Ma, K. Zhang, X. Liang, Y. Shen, F. Nan, F. Yi, V.C. Luca, J. Zhou, C. Jiang, J. Sun, X. Xie, X. Yu, Y. Zhang, Structural basis of bile acid receptor activation and Gs coupling, BioRxiv. 05 (2020) https://doi.org/10.1101/2020.05.24.104034, 24.104034.

[38] S.C. Lim, J.E. Choi, H.S. Kang, S.I. Han, Ursodeoxycholic acid switches oxaliplatin-induced necrosis to apoptosis by inhibiting reactive oxygen species production and activating p53-caspase 8 pathway in HepG2 hepatocellular carcinoma, Int. J. Cancer 126 (2010) 1582–1595.

[39] E. Sievanen, Exploitation of bile acid transport systems in prodrug design, Molecules. 12 (2007) 1859–1889.

[40] W. Liu, Q. Ye, J. Jiang, L. Lou, Y. Xu, C. Xie, M. Xie, cis-[Pt(II) (1R,2R-DACH)(3-acetoxy-1,1-cyclobutanedicarboxylato)], a water-soluble, oxalate-free and stable analogue of oxaliplatin: synthesis, characterization, and biological evaluations, Chem. Med. Chem. 8 (2013) 1465–1467.

[41] L. Gamelin, M. Boisdron-Celle, R. Delva, V. Guerin-Meyer, N. Ifrah, A. Morel, E. Gamelin, Prevention of oxaliplatin-related neurotoxicity by calcium and magnesium infusions: a retrospective study of 161 patients receiving oxaliplatin combined with 5-fluorouracil and leucovorin for advanced colorectal cancer, Clin. Cancer Res. 10 (2004) 4055–4061.

[42] L. Gamelin, O. Capitain, A. Morel, A. Dumont, S. Traore, L.B. Anne, S. Gilles, M. Boisdron-Celle, E. Gamelin, Predictive factors of oxaliplatin neurotoxicity: the involvement of the oxalate outcome pathway, Clin. Cancer Res. 13 (2007) 6359–6368.

[43] J.J. Wilson, S.J. Lippard, Synthetic methods for the preparation of platinum anticancer complexes, Chem. Rev. 114 (2014) 4470–4495.

[44] K. Wu, J. Ding, C. Chen, W. Sun, B.F. Ning, W. Wen, L. Huang, T. Han, W. Yang, C. Wang, Z. Li, M.C. Wu, G.S. Feng, W.F. Xie, H.Y. Wang, Hepatic transforming growth factor beta gives rise to tumor-initiating cells and promotes liver cancer development, Hepatology. 56 (2012) 2255–2267.

[45] W. Liu, X. Chen, Q. Ye, Y. Xu, C. Xie, M. Xie, Q. Chang, L. Lou, A novel water-soluble heptaplatin analogue with improved antitumor activity and reduced toxicity, Inorg. Chem. 50 (2011) 5324–5326.

[46] W. Liu, X. Chen, Q. Ye, S. Hou, L. Lou, C. Xie, 3-Hydroxy-carboplatin, a simple carboplatin derivative endowed with an improved toxicological profile, Platin. Met. Rev. 56 (2012) 248–256.

[47] Y. Yu, L. Lou, W. Liu, Q. Ye, S.Q. Hou, Synthesis and anticancer activity of lipophilic platinum(II) complexes of 3,5-diisopropyl salicylate, Eur. J. Med. Chem. 43 (2008) 1438–1443.

[48] B.Q. Li, X. Dong, S.H. Fang, J.Y. Gao, G.Q. Yang, H. Zhao, Systemic toxicity and toxicokinetics of a high dose of polyethylene glycol 400 in dogs following intravenous injection, Drug Chem. Toxicol. 34 (2011) 208–212.

[49] M. Boesjes, V.W. Bloks, J. Hageman, T. Bos, T.H. Dijk, R. Havinga, H. Wolters, J. W. Jonker, F. Kuipers, A.K. Groen, Hepatic farnesoid Xreceptor isoforms α2 and α4 differentially modulate bile salt and lipoprotein metabolism in mice, PLoS One 9 (12) (2014), e115028.

[50] Y. Chen, X.L. Song, L. Valanejad, A. Vasilenko, V.R. More, X. Qiu, W.K. Chen, Y. R. Lai, A.L. Slitt, M.A. Stoner, B.F. Yan, R.T. Deng, Bile salt export pump ss dysregulated with altered Farnesoid X receptor isoform expression in patients with hepatocellular carcinoma, Hepatology. 57 (2013) 1530–1541.

[51] J.N. Wu, J.R. Chen, J.L. Chen, Role of farnesoid X receptor in the pathogenesis of respiratory diseases, Can. Respir. J. 2020 (2020). Article ID 9137251.